SALSA is an ICT based educational tool for Astrophysics students to study structure and dynamics of Milky Way Galaxy

*

1st Mir Sakhawat Hossain
Department of Mathematics
Kabi Nazrul Government College
Dhaka, Bangladesh
s.hossain18@gmail.com

2nd Banrupa Mallik
Department of Physics
Begum Badrunnessa Govt. Girls College
Dhaka, Bangladesh
banrupamallik@gmail.com

***Abstract*—After the discovery of radiation from Galactic Hydrogen gas clouds in 1951 the 21cm wavelength HI line had become the best procedure to study spectral profiles in radio astronomy. It has utilized as an important tracer for the distribution and velocity of gas clouds in the Interstellar that has helped enormously to understand the galactic structure. On the other hand, ICT based Astronomy and Astrophysics tools have been being developed for decades. For undergraduate-level laboratory experiment, it can be assembled a radio frequency receiving system at a minimal cost which can be controlled through the Internet to study galactic structure and dynamics. This paper presents an observation to study galaxy dynamics and map its spiral structure which was carried out within galactic coordinate longitude 6° to 225° and latitude 0° to 35° with a low cost Haystack model type radio frequency receiving system 2.3 meter SALSA radio telescope at Onsala Space Observatory in Sweden maintained by Chalmers University of Technology. Components of the velocity of Hydrogen gas clouds were calculated using different galactic longitudes and latitudes as a function of galactic distance from the center to plot spiral galactic arms and rotation curve. This radio observational experiment was done by remote operation through the Internet in frequency switching mode. This project aims to prove quality and importance of this type of ICT based tools for astronomy education and citizen science.**

***Index Terms*—Open Educational Resources, STEM, Educational technology, Physics education, Student experiments**

I. Introduction

Neutral Hydrogen(HI) at the ground state level is abundant and uniformly distributed element throughout the interstellar medium(ISM). It is the most ubiquitous element in interstellar low-density regions but can be detected in $\lambda \approx 21$ cm or ≈ 1420 MHz where H_2 is symmetric but not detectable at the radio frequencies [1]. In 1933 Karl Guthe Jansky detected first extraterrestrial radio frequency [2]. After that in 45 Then Van de Hulst predicted 21 cm wavelength emission [3]. The same frequency line is also detected by Muller and Oort [4] in the same year. A preliminary survey was made by Christiansen and Hindman [5] in Australia. They made this survey with a 7.5-m paraboloid and movable radio antenna that had beam width between half power with direction of 1.9° horizontally and 2.7° vertically and it covered galactic longitude -10° to $+10^\circ$ at galactic plane. In Netherlands Muller and Westerhout [6] took an extended neutral HI line profile survey and made a catalog approximately in galactic latitude $\pm 20^\circ$ and longitude 318° to 220°. Within these periods angular resolution has been developed from 30° to 30-μas [7], [8]. Recently all-sky mapping in HI line based on EBHIS and GASS has been completed [9] with angular resolution $16.2''$ and sensitivity $\sigma_{rms} = 43$ mK. Santo and Ashraf carried out a galactic survey to map the Milky Way galaxy in galactic longitude 0° to 225° in galactic plane [10] using SALSA radio telescope which was built for EU HOU project [11]. Considering this observation we have accomplished our observation using the SALSA radio telescope in extended galactic coordinates i.e., galactic longitude 6° to 225° and latitude 0° to 35°. We have discussed here SALSA Radio Telescope, Basic block diagram of a SALSA type telescope, galactic geometry for observable parameters, observation details, data analysis and results with plotting and importance of this project.

Chalmers University of Technology, Onsala, Sweden.

II. SALSA Radio Telescope

A. Basic Details of SALSA

SALSA is a part of the European Hands-On Universe project(EU-HOU) [12] to bring interactive lessons of astronomy to the classroom [13]. There are two SALSA telescopes with the same specification see Table I [14]. Anyone can control these telescopes using Internet browser by log in https://vale.oso.chalmers.se/salsa/ for free at any time.

The telescope is composed of several main components:

- A 2.3 meter satellite dish on a fully steerable, motorized azimuth-elevation mount
- A rotor controller to run the motors which steer the telescope
- A feed composed of a helical antenna backed by a cavity

TABLE I
SPECIFICATION OF SALSA

Parameter	Value
Diameter	2.3 m
Focal length	0.9 m (f/0.37)
Angular resolution	7 degree at 1420 MHz
Frequency range	1420 $\pm$ 20 MHz
Frequency resolution	9.375 kHz (2.4 MHz over 256 frequency channels)
Noise diode temperature	$\approx$ 100K
System temperature	$\approx$ 500K
Aperture efficiency	$\approx$ 50%
Mount	two-axis azimuth/elevation
Pointing accuracy	$\approx$ 0.2 degree
Travel limits	0-90° vertically, 0-360° horizontally

- A super-heterodyne receiver providing 10 MHz bandwidth centered on the 1420.4 MHz (21-cm) hydrogen line
- A low-noise amplifier
- A/D conversion on a dedicated PCI card
- Software on a desktop computer to receive and process data from the telescope and control it

This components are the same as Haystack small radio telescope [15].

B. Basic Diagram of a Small Radio Telescope

SALSA block diagram is the same as Haystack model see Figure 1 shows the block diagram of the entire radio system, with fundamental elements, theoretical gain and attenuation of signal for each stage and see Table II is a summery of key data of this system [15].

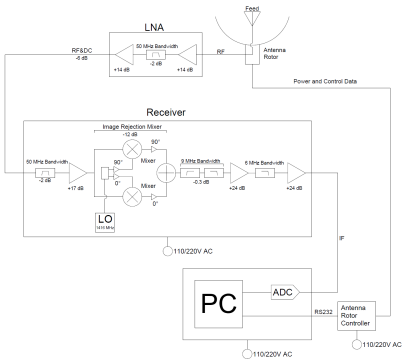

Fig. 1. Block Diagram of Haystack Small Radio Telescope

III. THEORY

A. Hyperfine Splitting of Hydrogen

Neutral Hydrogen consists of a motionless proton(positively charged $+e$) and moving electron(negatively charged $-e$) see Figure 2. Electron orbits around the proton for the mutual attraction of opposite charges. The derivation is as follows

TABLE II
KEY DATA FOR HAYSTACK SMALL RADIO TELESCOPE

Parameter	Value
Theoretical gain	71 dB
Measured gain	71.5 dB
HPBW	6.5°
Feed S11	-23.5 dB
System temperature	171 K

Griffiths [16]. We can imagine electron is orbiting around nucleus(proton). From the view of an electron, the proton is orbiting electron. This circling creates a magnetic field $\vec{B}$ in the frame of an electron which causes a torque on the spinning electron. It has a tendency to align its magnetic moment($\vec{\mu}$) along the direction of magnetic field [16]. So Hamiltonian (1)

$$H = -\vec{\mu} \cdot \vec{B} \tag{1}$$

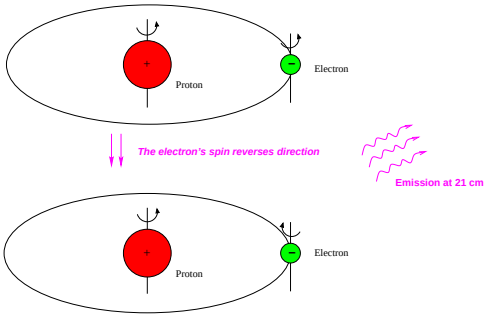

Fig. 2. An illustration of the 21cm transition of the hydrogen atom, caused by the energy change when the electron's spin changes from parallel to the proton's spin to antiparallel [17].

We can calculate magnetic field of a proton($\vec{B}$) and dipole moment of an electron($\vec{\mu}$) using Biot Savart law which is (2)

$$B = \frac{\mu_0 I}{2r} \tag{2}$$

Moreover magnetic field $\vec{B}$ and angular momentum $\vec{L}$ are in the same direction, so (3)

$$\vec{B} = \frac{1}{4\pi\epsilon_0} \frac{e}{mc^2 r^3} \tag{3}$$

The direction of magnetic moment $\vec{\mu}$ and spin $\vec{S}$ are the same, so (4)

$$\vec{\mu} = \frac{q}{2m}\vec{S} \tag{4}$$

If e is charge of electron, m_e is mass of electron and $\vec{S}_e$ is spin of electron then magnetic moment of electron is (5),

$$\vec{\mu}_e = -\frac{e}{m_e}\vec{S}_e \tag{5}$$

If m_e is mass of proton, $\vec{S}_e$ is spin of proton and $\vec{g}_p$ is g-factor (measured value is 5.59) then magnetic moment of proton is (6),

$$\vec{\mu}_e = \frac{g_p e}{2m_p}\vec{S}_p \tag{6}$$

In accordance with classical electrodynamics, the magnetic field produced by dipole $\vec{\mu}$ of the proton sets up magnetic field (7)

$$\vec{B} = \frac{\mu_0}{4\pi r^3}[3(\vec{\mu}\cdot\hat{r})\hat{r} - \vec{\mu}] + \frac{2\mu}{3}\vec{\mu}\delta^3(\vec{r}) \tag{7}$$

So Hamiltonian of the electron in the magnetic field due to magnetic dipole moment of proton is (8)

$$\vec{H}'_{hf} = \frac{\mu_0 g_p e^2}{8\pi m_p m_e}\frac{[(3\vec{S}_e\cdot\hat{r})(\vec{S}_e\cdot\hat{r})] - \vec{S}_p\cdot\vec{S}_e}{r^3} + \frac{\mu_0 g_p e^2}{3m_p m_e}\vec{S}_p\cdot\vec{S}_e\delta^3(\vec{r}) \tag{8}$$

In accordance with perturbation the first order correction is the expectation value of the perturbing Hamitonian (9)

$$E^1_{hf} = \frac{\mu_0 g_p e^2}{8\pi m_p m_e}\left\langle\frac{[(3\vec{S}_e\cdot\hat{r})(\vec{S}_e\cdot\hat{r})] - \vec{S}_p\cdot\vec{S}_e}{r^3}\right\rangle + \frac{\mu_0 g_p e^2}{3m_p m_e}\left\langle\vec{S}_p\cdot\vec{S}_e\right\rangle|\psi(0)|^2 \tag{9}$$

In the ground state level, the wave function is spherically symmetrical and the first expectation value vanishes. So we get (10)

$$E^1_{hf} = \frac{\mu_0 g_p e^2}{3\pi m_p m_e a^3}\left\langle\vec{S}_p\cdot\vec{S}_e\right\rangle \tag{10}$$

This is called spin-spin coupling because of the dot product of two spin $\vec{S}_p$ and $\vec{S}_e$. For this coupling the individual spin angular momenta are not conserved. So the good states are eigen vectors of total spin (11)

$$\vec{S} \equiv \vec{S}_e + \vec{S}_p \tag{11}$$

By applying total spin states the expected perturbation value can be written as terms of eigen operators as follows (12)

$$\vec{S}_p\cdot\vec{S}_e = \frac{1}{2}(S^2 - S_e^2 - S_p^2) \tag{12}$$

But both of electron and proton have spin $1/2$, so $S_e^2 = S_p^2 = (3/4)\hbar^2$. In the triplet state(parallel spins) total spin is 1 and so $S^2 = 2\hbar^2$. In the singlet state total spin is 0 and $S^2 = 0$. Thus (13)

$$E^1_{hf} = \frac{4g_p\hbar^4}{3m_p m_e^2 c^2 a^4}\begin{cases}+\frac{1}{4} & \text{(triplet)}\\ -\frac{3}{4} & \text{(singlet)}\end{cases} \tag{13}$$

The spin-spin coupling breaks the spin degeneracy of the ground state lifting the triplet configuration and depressing the singlet. The energy gap is evidently (14)

$$\Delta E = \frac{4g_p\hbar^4}{3m_p m_e^2 c^2 a^4} = 5.88\times10^{-6}eV \tag{14}$$

The frequency of the photon emitted in a transition from the triplet to the singlet state is (15),

$$\nu = \frac{\Delta E}{h} = 1420\,\text{MHz} \tag{15}$$

The corresponding wavelength is $c/\nu = 21$ cm which is a part of micro wave region [10], [16]. In a single Hydrogen atom this transition occurs once per $\approx 10^7$ years but enormous amount of Hydrogen in spiral arms of Milky Way galaxy causes pervasive and ubiquitous forms of radiation which is observable by radio telescope [10].

B. Geometry of Galaxy

The simplified geometry of the Milky Way galaxy [18] see Figure. 3

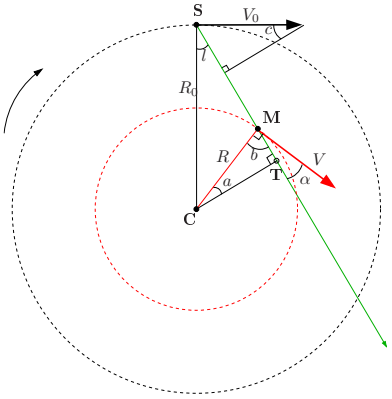

Fig. 3. Geometry of the Galaxy. C is the location of the Galactic center, S that of the Sun, M that of a gas cloud that we want to observe. The SM line is the line-of-sight. The arrow on an arc indicates the direction of rotation of the Galaxy. The arrows on line segments indicate the velocity of the Sun ($\vec{V}_0$) and the gas cloud ($\vec{V}$) [18].

There may be a lot of Hydrogen gas clouds in this direction, but for the purpose of this derivation we only care about a single cloud located at position M see Figure. 3. Since both the Sun and the cloud are moving, we do not evaluate the cloud velocity directly. Instead, we measure the relative velocity, $\vec{V}_r$, between us and the cloud, projected on the line-of-sight [18]. Since the observation of Hydrogen gas clouds located at tangential points of galactic plane at different longitudes, the radial velocity of the gas clouds can be written as (16),

$$\vec{V}_r = \vec{V}\cos\alpha - \vec{V}_0 \sin c \tag{16}$$

Where $\vec{V}$ is the velocity of gas clouds and $\vec{V}_0$ is the velocity of the Sun around galactic center. This equation can be simplified as equation (17),

$$\vec{V}_r = \vec{V}\frac{R_0}{R}\sin l - \vec{V}_0 \sin l \tag{17}$$

This equation is for all galactic longitude l. Here R_0 is distance between Sun and galactic center, R is distance between (HI) gas cloud and galactic center. We now assume that gas in Milky Way obeys differential rotation, i.e. the rotational speed is constant with radius and is the same as the rotational speed of the Sun, i.e. equation (18)

$$\vec{V}_r = Constant = \vec{V}_0 \tag{18}$$

With this assumption we can write from equation (17) we can simplify as a function of cloud distance R and $\vec{V}_r$ as follows equation (19)

$$R = \frac{R_0 \vec{V}_0 \sin l}{\vec{V}_0 \sin l + \vec{V}_r} \tag{19}$$

From measurement of radial velocity $\vec{V}_r$ we have calculated distance of gas cloud to the galactic centre. With the assumption of $R_0 = 8.5\,\mathrm{kpc}$ and $\vec{V}_0 = 220\,\mathrm{km\,s^{-1}}$, we can calculate value of R for different values of galactic longitude l. From Figure. 3 we can see that in the Quadrants I or IV there can be two possible locations corresponding to given values of l and R to us than the tangential point T (the actual point M on the Figure. 3), or farther away, at the intersection of the ST line and the inner circle. But in the Quadrants II or III position of the emitting gas clouds can be determined uniquely [18]. By the law of cosine in triangle in **CSM** we have equation (20),

$$R^2 = R_0^2 + r^2 - 2R_0 r\cos l \tag{20}$$

This is a second-order equation in r where r is distance to cloud from the Sun. The above equation has two possible solutions $r = r_+$ and $r = r_-$ that can be written as (21)

$$r\pm = \pm\sqrt{R^2 - R_0^2\sin^2 l} + R_0\cos l \tag{21}$$

From equation (21) we have discarded negative values and accepted one positive and two positive values. For convenient way of plotting to map the Milky Way structure, we convert the polar coordinate positions given as r and l to Cartesian $\mathbf{x} - \mathbf{y}$ coordinates using positive and negative values by 22

$$\begin{cases} x = r\cos(l - 90^\circ) \\ y = -R_0 + r\sin(l - 90^\circ) \end{cases} \tag{22}$$

Here we have deducted R_0 in $\mathbf{y}$ values instead of adding to get image of rotation to fit the Wikipedia image of galactic coordinates and during plotting we converted values from degree to radian. By calculating the value of $\mathbf{x}$ and $\mathbf{y}$ for different velocities at different galactic longitudes l in a graph to plot the map of Milky Way galaxy [16], [18].

IV. Observations

This observation was made with SALSA Radio Telescope situated in Onsala Space Observatory, Sweden. This telescope was operated to collect raw data through Internet[1] from Dhaka, Bangladesh. There are two radio lab antennas called "Brage" and "Vale". We used both of them. Each antenna has a diameter 2.3-m dish. The angular resolution is 7° at (HI) radio frequency line($1420\,\mathrm{MHz}$). Bandwidth of the receivers is $2.5\,\mathrm{MHz}$ and 256 frequency channels. Width of each channel is $9.765\,\mathrm{KHz}$. The telescope is controlled by qradio software. The observation was completed in frequency switching mode with reference frequency $1422.9\,\mathrm{MHz}$ and gain factor 800 [18].

A. Data Reduction

The observation was made in galactic coordinate longitude 6° to 225° and latitude 0° to 35° following 3° for galactic longitudes and 5° for galactic latitudes. The spectra were collected with integration time $150 - 300\,\mathrm{seconds}$ for each. By observing radio emission from galaxy Hydrogen, we have come to know about the motion of Hydrogen gas clouds around the Milky Way galaxy. We have used the Doppler effect to relate observed frequency spectra to the velocity of emitting Hydrogen gas clouds. By the equation of Doppler shift [18] we get (23)

$$\frac{\mathbf{f} - \mathbf{f}_0}{\mathbf{f}_0} = -\frac{\vec{v}}{\vec{c}} \tag{23}$$

Here $\mathbf{f}$ is the observed frequency, $\mathbf{f}_0$ is the rest frequency of line we are observing, v is the velocity of gas clouds(positive velocity for receding and negative velocity for approaching) and $\vec{c}$ is the velocity of light. Thus we converted frequency spectra to velocity scale then we corrected baselines. After that we applied Gaussian Fit function to smooth the spectra according to the equation (24)

$$\mathbf{y} = \sum_{i=1}^{n} \mathbf{a}_i e^{\left[-\left(\frac{\mathbf{x}-\mathbf{b}}{\mathbf{c}_i}\right)^2\right]} \tag{24}$$

Here $\mathbf{a}$ is the amplitude of spectra, $\mathbf{b}$ is the location of the centre of peak, $\mathbf{c}$ is the width of peak and n is the number of peaks to fit [18]. We collected peak values with SalsaJ software and SalsaSpectrum [19] MATLAB software class file. We have saved all the raw FITS files, Analysis codes, SalsaSpectrum class file and final plotted graphs in a data repository [20].

B. Result

The Gaussian Fit equation (24) has been applied to calculate the central velocity of the spectra. Then we used the equation (19) to calculate distance R of the clouds for different longitudes l. The values of R has been used to calculate r and checked whether it is single or double positive where we discarded negative values [10], [14]. We converted these values to the Cartesian coordinates and plotted these coordinates

[1]Website address of SALSA web based data collection facility is https://vale.oso.chalmers.se/salsa/welcome

to unravel the spiral structure of Milky Way Galaxy using MATLAB software of version R2017a. Here Perseus arm, Orion arm and other outer arms are clearly identified but some of them are not well recognizable. Here Map of Milky Way in Figure 4

Moreover we know that rotation curve is a function between circular velocity and radius. By using SALSA Telescope we can calculate the rotation curve of Milky Way [18]. We have calculated and plotted the rotation curve see Figure 5. Rotation curve of most galaxies which have solar systems shows flat rotation curve i.e. $\vec{V}(R)$ does not depend on R beyond certain radius. Angular velocityΩ varies as $\frac{1}{R}$. Matter near galactic center rotates with a larger angular speed than matter of farther away. But for larger radii this velocity is significantly larger than Keplerian case [18]. The figures we have got indication of existence of dark matter see Figure 5

V. Limitations and Errors

For the cause of small diameter of SALSA Telescope it reduces sensitivity and resolution. But they have strong and sensitive receiver and so detected important signals but could not detect the weaker (HI) signals from lower density areas. Below 6° and above 225° was not possible to observe for geographical position of telescopes. For this reason we could not observe the whole spiral structure of the Milky Way galaxy. There may be found errors in measuring central velocity of raw spectra [10], [18].

VI. Importance of this Experiment

The aim of this experiment is to describe how Astrophysics students who are actually amateur level astronomers can evaluate galaxy dynamics and detect existence of dark matter in our galaxy easily with small radio telescope. This kind of practice can educate educators, students and enthusiasts. In fact, radio astronomy had become popular by some amateur level astronomers by detecting signals from the galaxy. Cost effective instruments can be utilized to do amateur experiments because professional observatories are tightly scheduled for high-level scientific experiments. Professional Astronomers use high sensitive radio astronomical instruments to concentrate for a short time. But amateur level astronomers can do that for a long time. There are many amateur level radio clubs are doing some important projects like solar flare disturbance detection. Even citizen scientists can contribute to discover new things which can be slipped by professional scientists. So this kind of experiment has importance for both of education and research purposes. For Physics students, the galactic structure is important to learn the dynamics of galaxies and galactic dark matter detection. Students will need to be able to learn different types of coordinates, maps and coordinate transformations according to celestial reference systems. There are two types of techniques are applied and they are imagining and non-imaging. Observation of planetary radio signals, collecting solar flare data, meteor shower counts, GNSS satellite tracking, x-ray solar bursts etc. are included in non-imaging. They will learn also about imaging techniques, signal processing and collecting data from raw radio data sources with computer programming. Since an astrophysical observatory has many complex instruments, and if automated, it is a good example of automation for STEM students. By this way, students will learn about radio astronomy, physics, mathematics, computer programs etc.

VII. Conclusions

We have observed the Milky Way galaxy within galactic longitudes 6° to 225° and latitudes 0° to 3° successfully and mapped it with rotation curves which prove the existence of dark matter. It matched with previous observations. The spiral structure is clearly detectable in maps. In future, we will observe with a larger professional radio telescope for an all-sky survey to understand the 3D structure of Milky Way and its properties with higher sensitivity and higher resolution.

Acknowledgment

We are grateful to Onsala space observatory and the Chalmers University of Technology for their cooperation to carry out this survey. Special thanks to Eskil Varenius who was a supervisor of SALSA Radio Telescope. He helped us a lot to operate this telescopes and provided important information about data collection, data reduction, and analysis.

References

References

[1] "The hi 21 cm line," Website, Mar. 2016. [Online]. Available: https://www.cv.nrao.edu/course/astr534/HILine.html

[2] K. G. Jansky, "Radio waves from outside the solar system," *Nature*, vol. 132, no. 3323, p. 66, jul 1933.

[3] H. C. v. d. H. C J Bakker, *Radiogolven uit het wereldruim*. s-Gravenhage : Martinus Nijhoff, 1945.

[4] C. A. Muller and J. H. Oort, "Observation of a line in the galactic radio spectrum: the interstellar hydrogen line at 1,420 mc./sec., and an estimate of galactic rotation," *Nature*, vol. 168, no. 4270, p. 357, 1951.

[5] W. N. Christiansen and J. V. Hindman, "A preliminary survey of 1420 mc/s. line emission from galactic hydrogen," *Australian Journal of Chemistry*, vol. 5, no. 3, pp. 437–455, 1952.

[6] C. A. Muller, G. Westerhout *et al.*, "A catalogue of 21-cm line profiles," *Bulletin of the Astronomical Institutes of the Netherlands*, vol. 13, p. 151, 1957.

[7] K. I. Kellermann and J. M. Moran, "The development of high-resolution imaging in radio astronomy," *Annual Review of Astronomy and Astrophysics*, vol. 39, no. 1, pp. 457–509, 2001.

[8] E. Middelberg and U. Bach, "High resolution radio astronomy using very long baseline interferometry," *Reports on Progress in Physics*, vol. 71, no. 6, p. 066901, may 2008.

[9] N. B. Bekhti, L. Flöer, R. Keller, J. Kerp, D. Lenz, B. Winkel, J. Bailin, M. Calabretta, L. Dedes, H. Ford *et al.*, "Hi4pi: a full-sky h i survey based on ebhis and gass," *Astronomy & Astrophysics*, vol. 594, p. A116, 2016.

[10] T. R. Santo and S. A. Uddin, "Mapping the spiral structure of the milky way galaxy at 21cm wavelength using the salsa radio telescope of onsala space observatory," *International Journal of Astronomy*, vol. 2, no. 3, pp. 37–42, 2013.

[11] R. Doran, R. Ferlet, A. I. Gómez de Castro, R. Hill, C. Horellou, L. Mankiewicz, A.-L. Melchior, M. Metaxa, and A. Zanazzi, "European hands-on universe," in *European Planetary Science Congress 2007*, Aug. 2007, p. 940. [Online]. Available: http://adsabs.harvard.edu/abs/2007epsc.conf..940D

[12] R. Ferlet and C. R. Pennypacker, "The hands-on universe project," in *Organizations and Strategies in Astronomy Volume 6*. Springer Netherlands, 2006, pp. 275–286.

[13] O. S. Observatory, "Welcome to salsa," Website, May 2018. [Online]. Available: https://vale.oso.chalmers.se/salsa/welcome

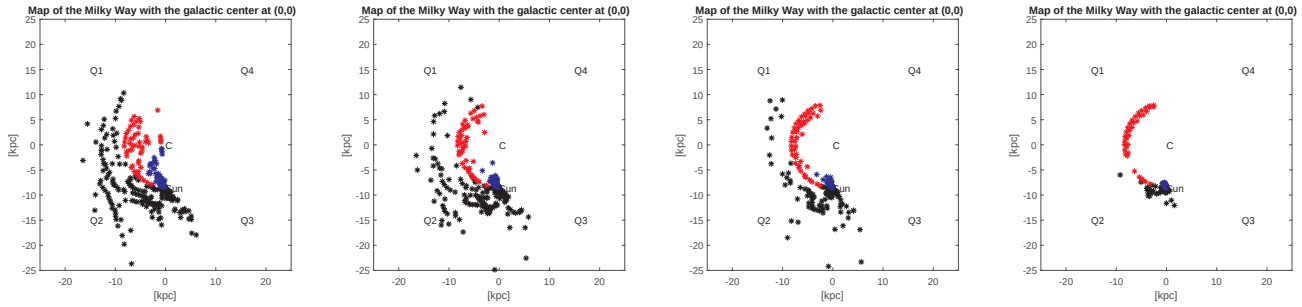

(a) $l = 6° - 225°$ and $l = 0°$ (b) $l = 6° - 225°$ and $l = 5°$ (c) $l = 6° - 225°$ and $l = 10°$ (d) $l = 6° - 225°$ and $l = 15°$

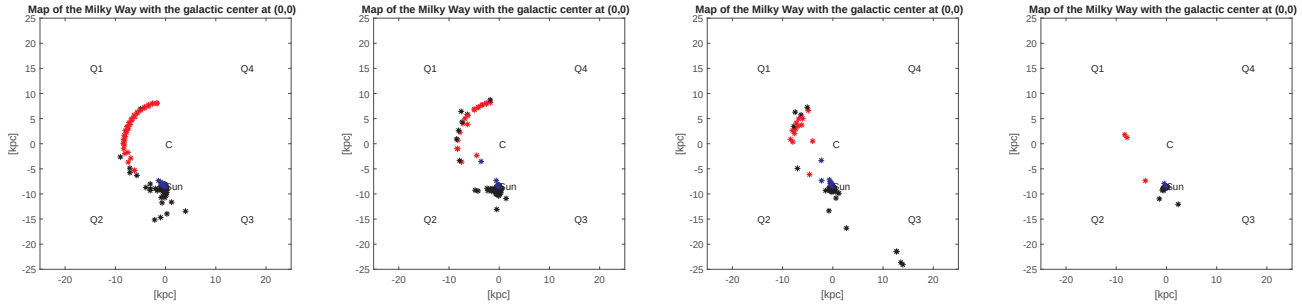

(e) $l = 6° - 225°$ and $l = 20°$ (f) $l = 6° - 225°$ and $l = 25°$ (g) $l = 6° - 225°$ and $l = 30°$ (h) $l = 6° - 225°$ and $l = 35°$

Fig. 4. Map of Milky Way at Galactic longitude(l) and Galactic longitude(b)

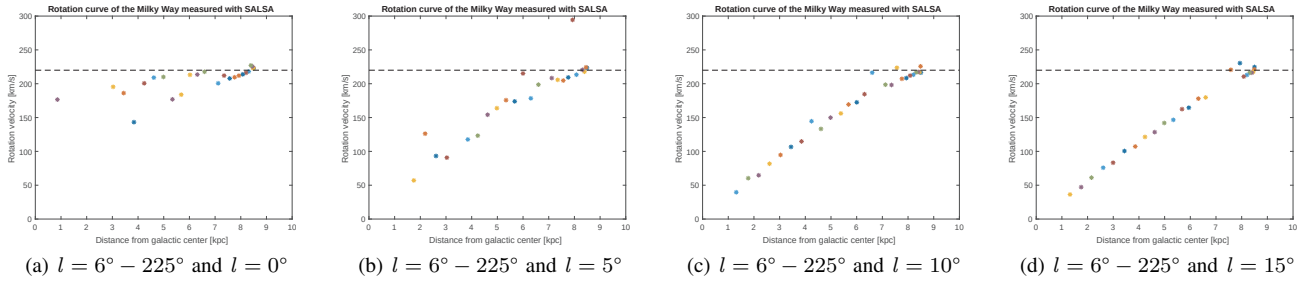

(a) $l = 6° - 225°$ and $l = 0°$ (b) $l = 6° - 225°$ and $l = 5°$ (c) $l = 6° - 225°$ and $l = 10°$ (d) $l = 6° - 225°$ and $l = 15°$

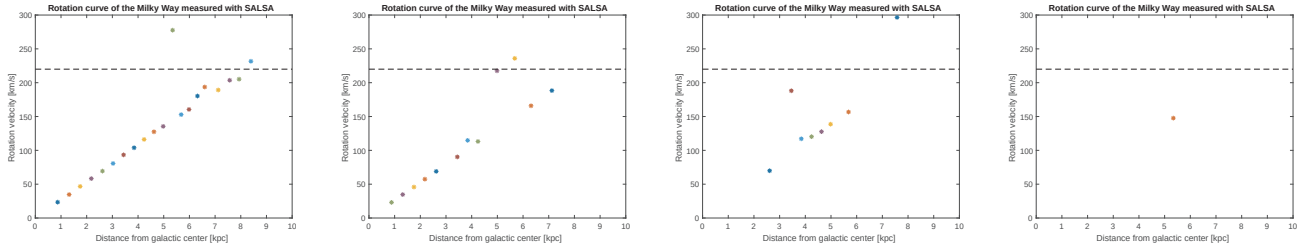

(e) $l = 6° - 225°$ and $l = 20°$ (f) $l = 6° - 225°$ and $l = 25°$ (g) $l = 6° - 225°$ and $l = 30°$ (h) $l = 6° - 225°$ and $l = 35°$

Fig. 5. Rotation Curve of Milky Way at Galactic longitude(l) and Galactic longitude(b)

[14] G. K. Thomas Bensby, *ASTA33 Lab: The rotation curve of the Milky Way*, Lund Observatory, Dec. 2017. [Online]. Available: http://www.astro.lu.se/Education/utb/ASTA33/

[15] A. R. Dustin Johnson, "Development of a new generation small radio telescope," Haystack Observatory, techreport, 2012. [Online]. Available: https://www.haystack.mit.edu

[16] D. J. Griffiths, *Introduction to quantum mechanics*. Cambridge University Press, 2016.

[17] "I.s.i.s. dante alighieri gorizia," Website, 2014. [Online]. Available: http://www.isisalighieri.go.it/

[18] D. J. Cathy Horellou and E. Varenius, "Salsa project documentation: Mapping the milky way," Online, Dec. 2015. [Online]. Available: https://github.com/varenius/salsa/

[19] E. V. Daniel Dahlin, *Reducing data from SALSA in Matlab-SalsaSpectrum*, Jun. 2015. [Online]. Available: https://vale.oso.chalmers.se/salsa/software

[20] M. S. Hossain, "Mapping the Milky Way at 21 cm Wave Length with SALSA Radio Telescope," Feb. 2018.